Article

## Universal Optical Conductance of Graphite

KUZMENKO, Alexey, *et al*.

**Abstract**

We find experimentally that the optical sheet conductance of graphite per graphene layer is very close to $(\pi/2)e2/h$, which is the theoretically expected value of dynamical conductance of isolated monolayer graphene. Our calculations within the Slonczewski-Weiss-McClure model explain well why the interplane hopping leaves the conductance of graphene sheets in graphite almost unchanged for photon energies between 0.1 and 0.6 eV, even though it significantly affects the band structure on the same energy scale. The f-sum rule analysis shows that the large increase of the Drude spectral weight as a function of temperature is at the expense of the removed low-energy optical spectral weight of transitions between hole and electron bands.

Reference

UNIVERSITÉ
DE GENÈVE

# Universal Optical Conductance of Graphite

A. B. Kuzmenko, E. van Heumen, F. Carbone,* and D. van der Marel

*DPMC, University of Geneva, 1211 Geneva 4, Switzerland*
(Received 5 December 2007; published 20 March 2008)

We find experimentally that the optical sheet conductance of graphite per graphene layer is very close to $(\pi/2)e^2/h$, which is the theoretically expected value of dynamical conductance of isolated monolayer graphene. Our calculations within the Slonczewski-Weiss-McClure model explain well why the interplane hopping leaves the conductance of graphene sheets in graphite almost unchanged for photon energies between 0.1 and 0.6 eV, even though it significantly affects the band structure on the same energy scale. The $f$-sum rule analysis shows that the large increase of the Drude spectral weight as a function of temperature is at the expense of the removed low-energy optical spectral weight of transitions between hole and electron bands.

One of the most remarkable macroscopic manifestations of quantum mechanics is the appearance of a universal conductance $e^2/h$, where $e$ is the elementary charge and $h$ is the Planck constant, in various physical phenomena. This value appears in the quantum Hall effect [1,2], in the superconductor-insulator transition in two dimensions [3,4], and in 1D ballistic transport [5–7]. Notably, all of these observations have thus far been restricted to the dc transport. Monolayer graphene [8,9] represents an interesting example, where the optical, or ac, conductance due to optical interband transitions is expected to be frequency independent and solely determined by the same universal value [10–12] in a broad range of photon energies:

$$G_1(\omega) = G_0 \equiv \frac{e^2}{4\hbar} \approx 6.08 \times 10^{-5} \ \Omega^{-1} \qquad (1)$$

(index "1" refers to the real part). Quite remarkably, $G_1(\omega)$ does not depend on microscopic parameters that normally determine optical properties of materials. This is a consequence of the unusual low-energy electronic structure of monolayer graphene that features electron and hole conical bands meeting each other at the Dirac point [9]. This type of dispersion is qualitatively different from more common quadratic massive bands, as has been most convincingly demonstrated by a $E_n(B) \propto \text{sgn}(n)\sqrt{|n|B}$ field dependence of Landau levels [13–16].

The absolute value of the optical conductance in graphene, the determination of which is an experimentally challenging task, has not yet been reported. However, it is legitimate to ask whether the predicted universality can already be observed in the conventional bulk graphite. Here we experimentally show that the answer is affirmative and explain it using the classical Slonczewski-Weiss-McClure (SWMcC) band model of graphite [17].

Equation (1), apart from the numerical factor, follows from a simple dimensional analysis. When the chemical potential $\mu$ is zero, the conductance is given by the formula

$$G_1(\omega) = \frac{\pi e^2}{\omega} |\mathbf{v}(\omega)|^2 D(\omega) \left[ f\left(-\frac{\hbar\omega}{2}\right) - f\left(\frac{\hbar\omega}{2}\right) \right] \quad (2)$$

where $\mathbf{v}(\omega)$ is the velocity matrix element between the initial state with energy $-\hbar\omega/2$ and the final state with energy $\hbar\omega/2$, $D(\omega)$ is the 2D joint density of states, and $f(\epsilon) = [\exp(\epsilon/T) + 1]^{-1}$ is the Fermi-Dirac distribution. If only the nearest-neighbor hopping is present then $D_{i,f}(\omega) \propto \hbar\omega/t^2a^2$ and $|\mathbf{v}_{i,f}(\omega)| \propto v_F \propto ta/\hbar$, where $a \approx 1.42$ Å is the interatomic distance, $t \approx 3$ eV is the hopping value, and $v_F \approx 10^6$ m/s is the Fermi velocity. Therefore the nonuniversal parameters $t$, $a$ as well as the frequency $\omega$ in Eq. (2) cancel and one obtains at zero temperature $G_1(\omega) \propto e^2/\hbar$. An interesting consequence of Eq. (1) is that the optical transmittance of a freestanding monolayer graphene sample is also frequency independent and is expressed solely via the fine structure constant $\alpha = e^2/\hbar c$:

$$T_{\text{opt}} = \left(1 + \frac{\pi\alpha}{2}\right)^{-2} \approx 1 - \pi\alpha \approx 0.977 \qquad (3)$$

as follows from the Fresnel equations in the thin-film limit. The calculated conductance of undoped graphene is shown in Fig. 1(c) for several temperatures [18]. The depletion of the low-energy conductance with temperature is due to the gradual equilibration of the electron and hole occupation numbers close to the Fermi level. The "removed" optical spectral weight accumulates at zero frequency as a Drude peak (not shown), whose integrated intensity increases linearly with temperature [12,19]:

$$D_{\text{graphene}}(T) = \frac{e^2}{\hbar} T \ln 2. \qquad (4)$$

Optical measurements from 10 to 300 K were performed on highly ordered pyrolytic graphite (HOPG) of ZYA grade with the misorientation of the $c$ axis smaller than 0.4°. The samples were cleaved right before being inserted into a cryostat. Reflectivity at near-normal incidence $R(\omega)$ was measured from 2 meV to 0.8 eV using a Fourier transform spectrometer (Fig. 2). The absolute value was
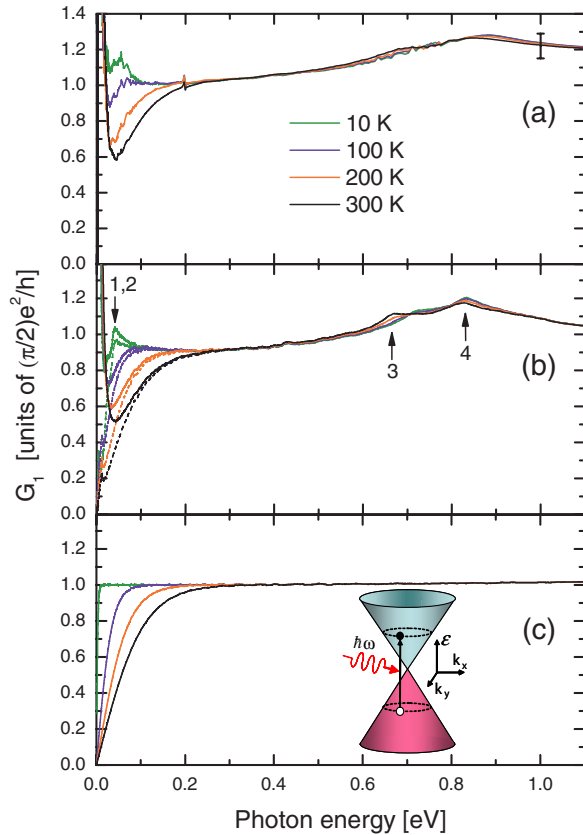
FIG. 1 (color online).   The real part of the optical sheet conductance of graphite per layer [(a) experiment, (b) calculation)] as well as the calculated conductance of isolated undoped graphene (c). The error bar indicates the inaccuracy of the absolute value due to systematic experimental uncertainties; the relative inaccuracy of the temperature dependence is much smaller. In (b) the dashed lines indicate the interband conductance only, while the solid line represents the total conductance with a Drude peak added (the scattering rate is 5 meV). In (c) the thermally activated Drude peak is not shown. The arrows in (b) correspond to optical transitions indicated in Fig. 3. A certain noise in (b) and (c) is of numerical origin. The inset of (c) depicts the optical transitions between hole and electron bands in monolayer graphene.

obtained by *in situ* gold evaporation. Our reflectivity spectra are in agreement with previous measurements [20–22]. In the range 0.7–4.5 eV, we extracted the real and imaginary parts of the dielectric function from ellipsometric measurements (shown in the inset). The correction for the admixture of the interplane optical component to the ellipsometry spectra was initially performed using the $c$-axis dielectric function found in Ref. [23] and refined by comparing the reflectivity and ellipsometric spectra in the range where they overlap. The uncertainty due to this procedure is the main source of the error bar shown in Fig. 1(a). The complex in-plane conductivity $\sigma(\omega)$ in the whole range was derived using a Kramers-Kronig consistent procedure [24], where the phase of the complex reflectivity at low energies is anchored by ellipsometric data.
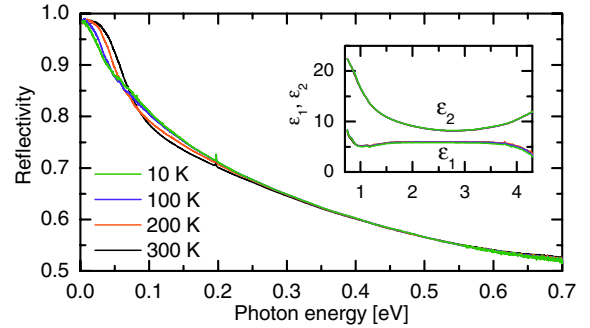


FIG. 2 (color online).   In-plane infrared reflectivity spectra of highly ordered pyrolytic graphite. The inset shows the real and the imaginary parts of the dielectric function obtained by ellipsometry at higher energies.

The sheet conductance per graphene layer was calculated using the relation $G(\omega) = d_c \sigma(\omega)$, where $d_c = 3.35$ Å is the interlayer distance. Importantly, the optical measurements reflect mostly bulk material properties, since the penetration depth is several tens of $d_c$.

Figure 1(a) shows the real part of the measured conductance of HOPG normalized by $G_0$. One can notice a remarkable similarity between these spectra and the calculated ones for graphene [1(c)]. The conductance is almost constant and close to $G_0$, especially between 0.1 and 0.6 eV. The second observation is that the conductance at low energies shows a strong depletion with increasing temperature in a fashion very similar to the temperature dependence of $G_1(\omega)$ in graphene. In contrast to the graphene spectra, the conductance of graphite shows a Drude peak below 10–20 meV, an extra structure at about 50 meV, and two broad peaks at about 0.7 and 0.9 eV. The small narrow peak at 0.2 eV is an optical phonon [25]. In general, we conclude that the universality of the conductance envisaged for the isolated graphene is also present in graphite in a broad energy range, in spite of the modification of the band structure by a significant $c$-axis hopping ($t_\perp \sim 0.3$–0.4 eV) [17]. This result is not trivial since the universal conductance is observed at energies of the order of $t_\perp$. For example, the calculated sheet conductance of bilayer graphene shows a strong frequency dependence caused by the interlayer hopping [26,27].

In order to understand this observation, we calculated infrared spectra of graphite with the standard $AB$-type stacking using a tight-binding Hamiltonian, which contains all hopping terms of the SWMcC model [17] and the on-site energy difference between the nonequivalent carbon atoms. In addition to the already mentioned in-plane nearest-neighbor hopping $t \approx 3$ eV, the model contains the interplane nearest-neighbor hopping ($t_\perp \approx 0.3$ eV) and several weaker terms corresponding to the next-nearest-neighbor orbital overlaps. The values of parameters, which were assumed to be temperature independent, were taken from Ref. [28]. The optical conductivity due to the direct interband transitions and the Drude spectral weight

were obtained using the standard relations, taking the temperature dependent occupation numbers into account. The four tight-binding bands of graphite in the vicinity of the *K-H* line are presented in Fig. 3. Near the *H* point the bands are conical, as in monolayer graphene, while they acquire a small mass, of the order of 5% of the free electron mass, as in double-layer graphene as one moves towards the *K* point. The lower and the upper bands disperse strongly along the *c* axis (by about 1.5 eV), while for the other two bands the dispersion is only 40 meV. This latter dispersion is responsible for the fact that the Fermi surface is electronlike at the *K* point and holelike at the *H* point. Overall, this picture is in agreement with the recent angle-resolved photoemission [29,30] and de Haas–van Alphen [31] measurements.

The in-plane conductance of graphite computed for this band structure is shown in Fig. 1(b). One can see that the simple band calculation is sufficient to understand the survival of the universal conductance value in the midinfrared range. There are two important factors that favor this. First, the energy of the Dirac point varies only weakly along the *K-H* line. We note that in doped graphene ($\mu \neq 0$) the conductance is gapped below $\omega = 2|\mu|$ [11]. The position of the Dirac energy with respect to the chemical potential changes from about $-20$ meV at the *H* point to
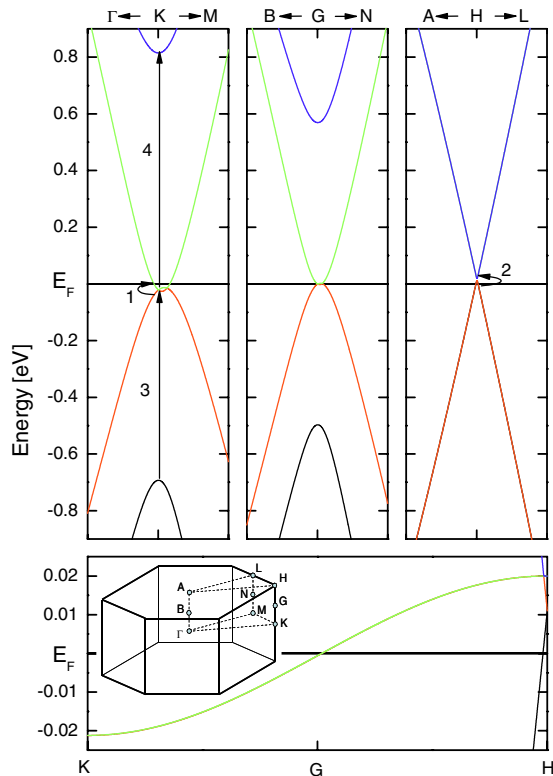
about 20 meV at the *K* point, which explains why the interband conductance precipitates dramatically below 40 meV (at $T = 0$) and forms a peaklike structure marked by 1 and 2. Importantly, this energy scale strongly depends on the type of stacking, since the stacking affects the dispersion of the Dirac point energy along the *c* axis. For example, a similar calculation on a hypothetical *AA*-stacked graphene (not shown here), where the same value of $t_\perp$ was taken, indicates that in this system the conductance would be strongly suppressed below 1.5 eV.

The second factor is a less obvious but equally essential one. The frequency-independent conductance can be easily explained only in the case of nonsplit conical bands, while in graphite the bands are split and slightly parabolic, except close to the *H* point. In fact, a partial conductance (not shown) calculated for all momentum states with a certain value of $k_z$ away from the *H* point has a strong frequency dependence, very similar to the expected conductance of bilayer graphene [26,27]. It shows a sharp double peak due to the transitions marked as 3 and 4 and a depletion at lower energies where only two bands out of four contribute to it. Essentially, the optical weight is redistributed by the *c*-axis hopping. However, in the total (i.e., the $k_z$ integrated) conductance this redistribution is almost averaged out, due to the fact that the splitting size changes continuously from the maximum value (0.7 eV for the transition 3 and 0.9 eV for the transition 4) at the *K* point to zero at the *H* point. Only close to the *K* point, where the bands show a van Hove singularity, these transitions make two broad conductance peaks 3 and 4 in Fig. 1(b) [20,21].

Finally, we study the redistribution of the optical spectral weight between different energy regions using the *f*-sum rule analysis. Symbols in Fig. 4 show the measured temperature dependence of the low-energy integrated conductance $W(\omega_c) = \int_0^{\omega_c} G_1(\omega)d\omega$ for $\omega_c = 12$ meV and 0.3 eV, respectively. The first one consists mostly of the Drude (intraband) spectral weight which strongly increases as a function of temperature due to the thermally excited electron-hole pairs. The second one contains both the Drude weight and the low-energy transitions between the hole and electron bands. The fact that it is practically independent of temperature proves that the Drude spectral weight is at the expense of the suppression of the low-lying interband conductance. The observed temperature dependence agrees nicely with the calculations in graphite (solid lines) described above. The absolute experimental values are somewhat higher than the ones predicted by the theory, which might be due to some underestimation of the Drude weight by the SWMcC model with the particular values of the hopping parameters used as well as due to the absolute experimental uncertainty of $G_1(\omega)$. For the purpose of illustration, we show on the same graph the calculated pure Drude spectral weight $D(T)$ of graphene [described by Eq. (4)] and of graphite, although it would not be trivial to extract this exact value from the experimental data, due to an overlap between the Drude peak and the interband transitions. One can see, however, that the calculated tem-



FIG. 3 (color online). The calculated dispersion of $p_z$ bands in graphite along the *K-H* line (along the *K'-H'* line the dispersion is the same). Different bands are shown with different colors. The arrows indicate interband transitions which form the correspondingly marked peaks in Fig. 1(b).
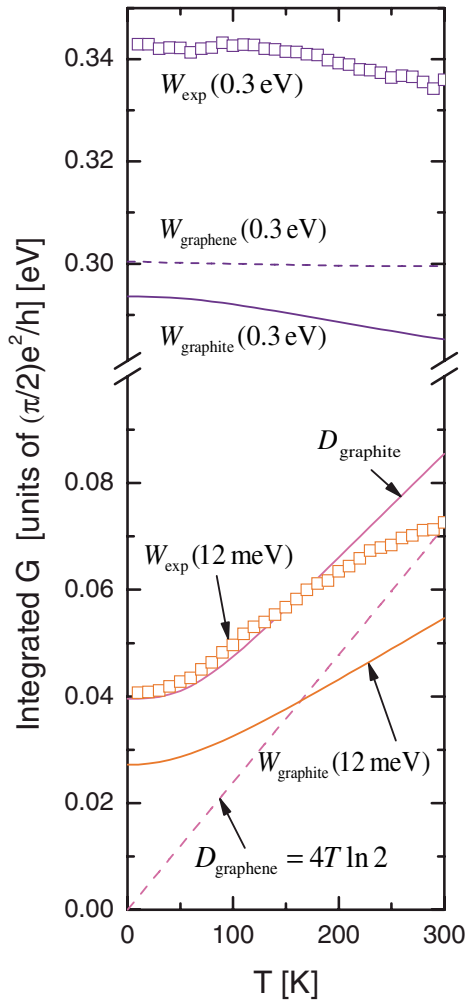
FIG. 4 (color online). The integrated conductance of graphite (symbols, experiment; solid lines, calculation) and of monolayer undoped graphene (dashed lines, calculation).

perature dependence of $W$ (12 meV) in graphite reflects well the one of the Drude weight alone.

In conclusion, our study reveals remarkable similarities between the measured optical conductance of highly ordered pyrolytic graphite per graphene layer and theoretical predictions for the monolayer graphene. First, the optical conductance of graphite due to the transitions between hole and electron bands is very close to the universal value of $e^2/4\hbar$ between 0.1 and 0.6 eV. Second, the optical spectral weight removed from the low-energy interband conductance at finite temperatures is transferred to the Drude peak. This implies that the low-energy charge dynamics in graphite is rather nontrivial as it involves simultaneously the Drude component and the transitions between the hole and electron bands.

*Present address: California Institute of Technology, Pasadena, CA 91125, USA.
[1] K. von Klitzing, G. Dorda, and M. Pepper, Phys. Rev. Lett. **45**, 494 (1980).
[2] R. B. Laughlin, Phys. Rev. B **23**, 5632 (1981).
[3] H. M. Jaeger, D. B. Haviland, A. M. Goldman, and B. G. Orr, Phys. Rev. B **34**, 4920 (1986).
[4] M. P. A. Fisher, G. Grinstein, and S. M. Girvin, Phys. Rev. Lett. **64**, 587 (1990).
[5] M. Buttiker, Y. Imry, R. Landauer, and S. Pinhas, Phys. Rev. B **31**, 6207 (1985).
[6] B. J. van Wees *et al.*, Phys. Rev. Lett. **60**, 848 (1988).
[7] D. A. Wharam *et al.*, J. Phys. C **21**, L209 (1988).
[8] K. S. Novoselov *et al.*, Science **306**, 666 (2004).
[9] A. K. Geim and K. S. Novoselov, Nat. Mater. **6**, 183 (2007).
[10] T. Ando, Y. Zheng, and H. Suzuura, J. Phys. Soc. Jpn. **71**, 1318 (2002).
[11] V. P. Gusynin, S. G. Sharapov, and J. P. Carbotte, Phys. Rev. Lett. **96**, 256802 (2006).
[12] L. A. Falkovsky and A. A. Varlamov, Eur. Phys. J. B **56**, 281 (2007).
[13] K. S. Novoselov *et al.*, Nature (London) **438**, 197 (2005).
[14] Y. Zhang *et al.*, Nature (London) **438**, 201 (2005).
[15] M. L. Sadowski, G. Martinez, M. Potemski, C. Berger, and W. A. de Heer, Phys. Rev. Lett. **97**, 266405 (2006).
[16] Z. Jiang *et al.*, Phys. Rev. Lett. **98**, 197403 (2007).
[17] J. W. McClure, Phys. Rev. **108**, 612 (1957); J. C. Slonzcewski and P. R. Weiss, Phys. Rev. **109**, 272 (1958).
[18] The calculations for monolayer graphene, shown in Figs. 1(c) and 4, take the finite bandwidth into account. However, in the shown frequency range, $G_1(\omega, T)$ almost coincides with $G_0[f(-\frac{\hbar\omega}{2}) - f(\frac{\hbar\omega}{2})]$, which is the result for perfectly conical bands.
[19] T. G. Pedersen, Phys. Rev. B **67**, 113106 (2003).
[20] E. A. Taft and H. R. Philipp, Phys. Rev. **138**, A197 (1965).
[21] G. Guizzetti *et al.*, Phys. Rev. Lett. **31**, 154 (1973).
[22] Z. Q. Li *et al.*, Phys. Rev. B **74**, 195404 (2006); The curves of $\sigma_1(\omega)$ shown in Fig. 1 of this reference were derived incorrectly from the reflectivity spectra as will be detailed in the forthcoming publication [Z. Q. Li and D. N. Basov (private communication)].
[23] D. L. Greenaway *et al.*, Phys. Rev. **178**, 1340 (1969).
[24] A. B. Kuzmenko, Rev. Sci. Instrum. **76**, 083108 (2005).
[25] L. J. Brillson *et al.*, in *Physics of Semimetals and Narrow-Gap Semiconductors*, edited by D. L. Carter and R. T. Bate (Pergamon, New York, 1971).
[26] D. S. L. Abergel and V. I. Fal'ko, Phys. Rev. B **75**, 155430 (2007).
[27] J. Nilsson, A. H. Castro Neto, F. Guinea, and N. M. R. Peres, Phys. Rev. Lett. **97**, 266801 (2006).
[28] B. Partoens and F. M. Peeters, Phys. Rev. B **74**, 075404 (2006).
[29] S. Y. Zhou *et al.*, Nature Phys. **2**, 595 (2006).
[30] A. Grüneis *et al.*, Phys. Rev. Lett. **100**, 037601 (2008).
[31] I. A. Lukyanchuk and Y. Kopelevich, Phys. Rev. Lett. **93**, 166402 (2004).